Resonant photoemission study of CeO_2

M. Matsumoto, K. Soda, K. Ichikawa, S. Tanaka, Y. Taguchi, K. Jouda, and O. Aita
College of Engineering, University of Osaka Prefecture, Gakuen, Sakai 593, Japan

Y. Tezuka and S. Shin
Institute for Solid State Physics, the University of Tokyo, Roppongi, Tokyo 106, Japan

(Received 12 May 1994)

The $4f$ electronic state and the decay process of the photoexcited $4d^9 4f^{n+1}$ states in CeO_2 are investigated by means of a resonant photoemission technique in the Ce $4d \rightarrow 4f$ photoabsorption region. Resonant enhancement of the valence-band emission is clearly observed in the giant-absorption region. This confirms the existence of the $4f$ electron in the ground state of CeO_2. The $4f$-derived emission exhibits a single-peak distribution rather than a double-peak structure such as observed in other Ce compounds. The Ce $5p$ emission band, which spreads over about 10 eV and consists of at least three or more fine structures, also shows the resonant enhancement in the giant-absorption region. In the prethreshold region, the Ce $5p$ fine structures as well as the $4f$ emission band show enhancements, but these constant-initial-state spectra are different from each other. The obtained results are discussed in terms of the mixed valence in the ground state of CeO_2 and of possible intermediate configurations in the resonant photoemission process.

I. INTRODUCTION

A Ce ion in an insulating CeO_2 has been nominally regarded as tetravalent with no $4f$ electron. The valence-band spectrum of CeO_2 studied by the x-ray photoelectron spectroscopy (XPS) reveals no isolated $4f$ photoemission peak,[1,2] while the spectrum of the CeO_2 sample reduced by sputtering and heating exhibits the $4f$ level 3 eV above the valence band, which mainly consists of the O $2p$ states.[3] The spectrum investigated by the bremsstrahlung isochromat spectroscopy (BIS) combined with the XPS study shows empty localized $4f$ states in the band gap.[3,4] In line with these results of the electron spectroscopic studies, the $4d \rightarrow 4f$ photoabsorption spectra of CeO_2 (Refs. 5–7) as well as the reflectance spectrum in the $4d \rightarrow 4f$ photoabsorption region[8] seem to support the $4f^0$ configuration in the ground state, since the overall profiles of the $4d \rightarrow 4f$ photoabsorption spectra resemble those of La trihalides with no $4f$ electron rather than those of Ce trihalides with one $4f$ electron. However, an energy-band calculation by Koelling, Boring, and Wood[9] which explains well the valence-band XPS and BIS spectra of CeO_2, has shown the $4f$ electron number of 0.5 and considerable covalent character in the O $2p$ valence band with the Ce $5d$ and $4f$ states. The detailed analyses of the $3d$ photoabsorption and photoemission spectra of CeO_2, based on an Anderson impurity model[4,10,11] or a cluster model,[12] have also pointed out that CeO_2 is strongly mixed valent between the $4f^0$ and $4f^1\underline{L}$ configurations in the ground state and that the average $4f$ electron number is about 0.5. Here, $\underline{L}$ denotes a hole in the valence band. Recently, it has been shown that the valence-band photoemission, BIS, and $4d$ photoabsorption spectra can be explained consistently with other core-level spectra in terms of the mixed valence in the ground state.[13–15]

Resonant photoemission has been extensively utilized for extracting the partial density of states such as the $3d$ state in transition-metal compounds and the $4f$ and $5f$ states in lanthanide and actinide compounds.[16–22] This resonant enhancement is caused by an indirect process, which has the same initial and final states as a direct photoemission process, associated with the Coster-Kronig or the super Coster-Kronig decay of the intermediate state reached by the photoabsorption. For instance, the $4f$ photoemission is resonantly enhanced at the $4d \rightarrow 4f$ photoexcitation due to the indirect process associated with the super Coster-Kronig decay

$$4d^{10}4f^1 + h\nu \rightarrow 4d^9 4f^2 \rightarrow 4d^{10}4f^0 + \epsilon l \ ,$$

where $h\nu$ and ϵl stand for an incident photon and an ejected photoelectron, respectively. The photon-energy dependence of the resonant enhancement is usually described in terms of the Beutler-Fano type profile.[23] The $4f$ partial density of states can be obtained by subtracting an off-resonance spectrum from an on-resonance spectrum. The enhancement of the $4f$ emission is so sharp and strong that even weak $4f$ emission such as in a dilute system $CeCu_6$[18–20] can be extracted by the use of the resonance. Allen briefly reported that the valence-band photoemission of CeO_2 exhibits resonant enhancement around the $4d$ threshold and suggested that the $4f$ emission is observed.[3] However, he did not discuss the valence-band spectrum in detail.

Furthermore, it has been recently observed that the magnitude of the resonance depends on the multiplets of the photoexcited $4d^9 4f^{n+1}$ states, i.e., the intermediate state in the indirect channel in the $4d \rightarrow 4f$ prethreshold absorption region in La trihalides[24,25] and Ce trihalides.[26] Here, n is the number of $4f$ electrons in the ground state. The $4f$ and $5p_{1/2}$ emission bands show peculiar photon-energy dependences. This has been successfully explained by the multiplet-dependence of the Auger transition probability involved in the resonance process and will be able to be utilized for elucidating the character of the excited state.[25,26]

In this paper, we report results of the 4*d*-4*f* resonant photoemission study of the valence and Ce 5*p* bands in CeO_2, in order to clarify the 4*f* electronic state and the excited states reached by the $4d \rightarrow 4f$ photoabsorption. We also reexamine the $4d \rightarrow 4f$ photoabsorption spectrum particularly in the prethreshold region by measuring the photoelectric yield in comparison with the recent theoretical investigation.[15] In the prethreshold region, multiplet structures due to the $4f^n \rightarrow 4d^9 4f^{n+1}$ electronic transition appear through the 4*d*-4*f* and 4*f*-4*f* Coulomb interactions in lanthanide compounds. Thus, the observed fine structures strongly reflect the initial 4*f* state.

II. EXPERIMENTAL PROCEDURES

Photoelectron measurements were carried out at the beamline 2 of SOR-RING, a 0.38-GeV electron storage ring, at the Synchrotron Radiation Laboratory, the Institute for Solid State Physics, the University of Tokyo. Light from the storage ring was monochromatized with a 2-m grazing-incidence monochromator of a Rowland-mount type. The spectral resolution was dependent on a photon energy and was about 0.3 eV at a photon energy of 102 eV with a 100-μm entrance slit and a 100-μm exit slit and a 120-groove/mm grating. Energy distribution of photoelectrons was measured with a double-stage cylindrical mirror analyzer (DCMA). The energy resolution of the analyzer was kept constant to 0.4 eV. Photoelectron spectra shown in this paper are normalized for the number of incident photons, but are not corrected for the transmittance of the DCMA.

We used two types of samples, i.e., single crystals and thin films evaporated *in situ* onto gold substrates. The single-crystalline CeO_2 was made with the use of a solar furnace and was used as a starting material for the evaporation as well. The thickness of the evaporated film was estimated to be about 100 Å with an oscillating-quartz thickness gauge. In the measurement on the single crystal, clean surfaces were prepared by scraping the specimen with a diamond file; a flood gun was used to minimize the effect of charging up.

The base pressure in a sample preparation chamber was about 10^{-8} Pa and rose to 10^{-6} Pa during evaporation. The pressure in the analyzer chamber was about 10^{-9} Pa during measurements.

III. RESULTS AND DISCUSSION

A. Photoelectric yield spectra

Figure 1 shows a total yield (TY) spectrum of the CeO_2 evaporated film and a partial yield (PY) spectrum of the CeO_2 single crystal in the Ce $4d \rightarrow 4f$ photoabsorption region. The details of the yield spectra in the Ce $4d \rightarrow 4f$ prethreshold absorption region are shown in Fig. 2. The PY spectrum was obtained by collecting photoelectrons with a kinetic energy of 19 eV. We also show TY spectra of LaF_3 and CeF_3 in these figures, where the TY spectrum of LaF_3 is shifted so that a peak observed at 97.5 eV in LaF_3 may line up with a peak observed at 103.5 eV in CeO_2. The Ce 4*d* direct photoemission contributes to the PY spectrum between 130 and 147 eV,[27,28] which results in the difference between the TY and PY spectra in that region. Except for this point, there is no qualitative

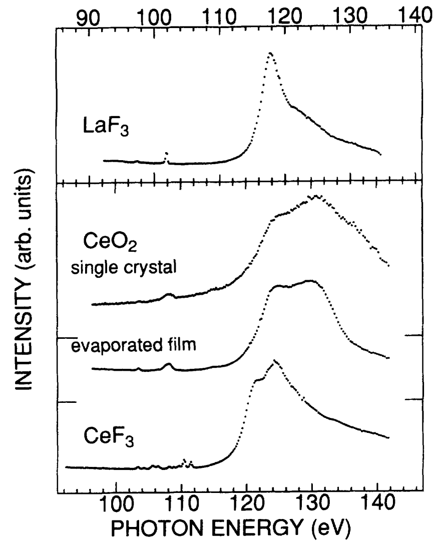

FIG. 1. Partial yield spectrum of single-crystalline CeO_2 and total yield spectra of evaporated films of CeO_2, LaF_3, and CeF_3 in the lanthanide $4d \rightarrow 4f$ absorption region. The spectrum of LaF_3 is represented so that a peak observed at 97.5 eV in LaF_3 may line up with a peak observed at 103.5 eV in CeO_2.

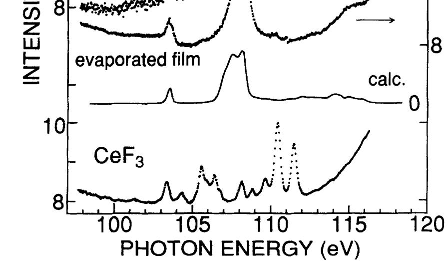

FIG. 2. Partial yield spectrum of single-crystalline CeO_2 and total yield spectra of CeO_2, LaF_3, and CeF_3 films in the lanthanide $4d \rightarrow 4f$ prethreshold absorption region. The spectrum of LaF_3 is represented so that a peak observed at 97.5 eV in LaF_3 may line up with a peak observed at 103.5 eV in CeO_2. The photoabsorption spectrum calculated by Kotani *et al.* (Ref. 15) is also shown by a solid line.

difference between the TY spectrum of the evaporated film and the PY spectrum of the single crystal. This indicates that the properties of samples do not change so much by evaporation. As seen in these figures, the yield spectrum of CeO_2, which shows the giant band and the peaks at 103.5 and 108 eV, is in close correspondence in shape with that of LaF_3 rather than that of CeF_3. However, the spectral features of CeO_2 are broader than those of LaF_3. Furthermore, weak structures are recognized around 105, 110, and 115 eV in the prethreshold region (Fig. 2). Although some of the weak structures are ambiguous in the PY spectrum of the single-crystalline CeO_2 because of the bad statistics, a broad feature is clearly observed at about 115 eV in both yield spectra.

In the photon-energy region where the $4d \rightarrow 4f$ photoabsorption takes place, we can consider both the TY and PY spectra as a $4d$ photoabsorption spectrum.[29] The overall profile of the yield spectra observed in the present study is similar to the $4d$ photoabsorption spectra of CeO_2 thin films obtained by Haensel, Rabe, and Sonntag,[5] Zimkina and Lyakhovskaya,[6] and Hanyuu *et al.*,[7] and the reflectance spectrum of a single-crystalline CeO_2 measured by Miyahara *et al.*[8] However, the fine structures in the prethreshold region are slightly different from those in the previous results, except for peaks observed at 103.5 and 108 eV. Some researchers attributed the fine structures other than the 103.5 and 108-eV peaks to the reduction of the specimen and considered them as extrinsic.[7] Some ignored the presence of the broad structure around 115 eV due to their emphasis on the similarity between the spectra of CeO_2 and La trihalides.[7,8] In the present study for the evaporated film, a trace of the trivalent Ce ion is observed in the valence-band photoelectron spectrum as will be described later, but the amount of the trivalent component is estimated to be very small. Furthermore, the broad feature is clearly observed in CeO_2 around 115 eV, where there is no structure in CeF_3. The integrated intensity of the broad structure is comparable to those of the 103.5 and 108-eV peaks, and is at least larger than that of the 103.5-eV peak. Thus, we consider at least the structure around 115 eV as intrinsic for CeO_2 as well as the 103.5 and 108-eV peaks.

The theoretical analyses[11,15] based upon the Anderson impurity model suggest that fine features appear on the high-energy side of the 108-eV peak. The theoretical photoabsorption spectrum in the prethreshold region of CeO_2 calculated by Kotani *et al.*[15] is also shown by a solid line in Fig. 2. It reproduces the present experimental results considerably well. According to the theoretical study, the peaks at 103.5 and 108 eV correspond to the transitions to the discrete $^3P_1$ and $^3D_1$ levels of the $4d^94f^1$ excited states, respectively, which are broadened by the hybridization with the quasicontinuum $4d^94f^2\underline{L}$ excited states, and structure due to the transition to the $4d^94f^2\underline{L}$ excited state spreads over 8 eV around 115 eV.

B. 4f emission

Figure 3 shows a series of energy distribution curves (EDC's) of the CeO_2 evaporated film measured at various photon energies around the Ce $4d$ threshold. Excitation photon energies are indicated on the right-hand side of each EDC. Binding energies are given relative to the Fermi level of gold. There are three photoemission bands corresponding to the Ce $5s$, Ce $5p$ (overlapped with the O $2s$ level) core levels, and valence band (denoted by VB in Fig. 3), as labeled on the spectrum taken at the 129.3-eV photoexcitation. Arrows $A-C$ indicate positions of constant kinetic energies, which correspond to the $N_{4,5}O_{2,3}O_{2,3}$, $N_{4,5}O_{2,3}V$, and $N_{4,5}VV$ Auger peaks, respectively. The shape of the valence band taken at the nonresonance photon energy is similar to those reported so far in the XPS studies.[1-4] We also measured EDC's for the CeO_2 single crystal (results are not shown). Unfortunately, we observed the effect of charging up, i.e., broadening of photoemission bands and their shift to the high binding-energy side, which depend on the photon energy and incident photon intensity. For films, such charging-up effects were not recognized. Then we will present results only for the evaporated film below.

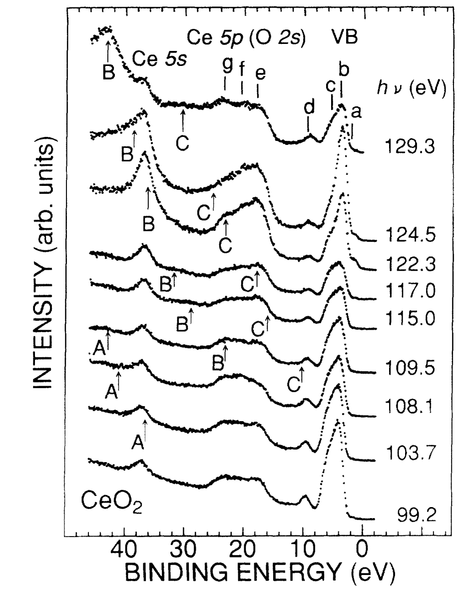

FIG. 3. Energy distribution curves for a CeO_2 evaporated film measured at various photon energies around the Ce $4d$ threshold. The excitation photon energies are indicated on the right-hand side of each spectrum. Binding energies are given relative to the Fermi edge estimated from the photoemission spectra of gold. Arrows $A-C$ indicate the peak positions where the Auger lines may appear.

In Fig. 3, we find four features $a-d$ in the valence-band region and at least three peaks $e-g$ in the Ce $5p$ band region. These features show the resonant enhancement at the $4d \rightarrow 4f$ photoexcitation as seen in the EDC at the 124.5-eV photoexcitation. In order to elucidate their photon-energy dependences, we show the constant-initial-state (CIS) spectra for the features $a-d$ in Fig. 4 and those for the features $e-g$ in Fig. 5 together with the TY spectrum. The CIS spectrum for the main valence-band feature b is consistent with the observation by Allen.[3]

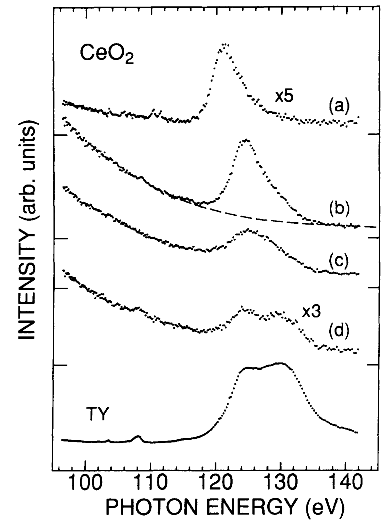

FIG. 4. Constant-initial-state spectra obtained at the binding energies of the features a–d in the valence-band photoemission spectra and a total yield spectrum of CeO_2. The ordinates of the spectra for the features a and d are magnified by factors of 5 and 3, respectively. The assumed photon-energy dependence of the nonresonant component is shown by a broken line.

The valence band in La trihalides with no $4f$ electron shows slight enhancement due to the La $5d$ and $6s$ components included in the valence band,[24] while the Ce $4f$ in Ce trihalides exhibits prominent enhancement in the $4d \rightarrow 4f$ giant-absorption region.[26,30] Recent research for some intermetallic Ce compounds in comparison with the conventional La counterpart has shown the fairly large Ce $5d$ contribution to the resonant enhancement of the valence band.[31] We cannot estimate the Ce $5d$ contribution to the resonance by simply adapting the same method, since there is no La counterpart, LaO_2, to be directly compared with, and the situation for insulating

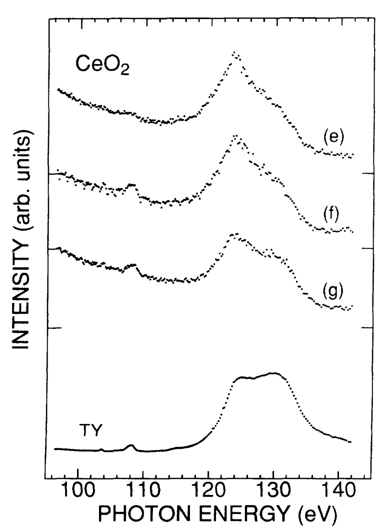

FIG. 5. Constant-initial-state spectra obtained at the binding energies of the features e–g in the Ce $5p$ band and a total yield spectrum of CeO_2.

CeO_2 is much different from the metallic compounds. In atomic Ce, however, it is known experimentally and theoretically that the Ce $4f$ CIS spectrum is quite different from CIS spectra of the other electrons such as the Ce $5d$ ones, which are less localized than the $4f$ electrons.[32,33] The $5d$, $5s$, and $5p$ CIS spectra show rather a symmetric profile for the resonance in the $4d \rightarrow 4f$ giant-absorption region, while the $4f$ CIS spectrum is asymmetric.[26,32,33] It shows a steep rise on the low photon-energy side of the resonance, and has a gentle decrease on the high photon-energy side. This dependence of the $4f$ enhancement on the photon energy has been ascribed to the localized nature of the $4f$ state.[32,33] Such difference has been also recognized between the $4f$ CIS spectrum of Ce trihalides and the valence-band CIS spectrum of La trihalides.[30]

Comparison between the obtained CIS spectra, especially between the CIS spectra of the main feature b, and of the shoulder c or the weak satellite a, shows that the main feature b in CeO_2 exhibits such an asymmetric enhancement at 125 eV as mentioned above. The overall profile of the CIS spectrum of the feature b for the resonance at the giant-absorption band resembles that of the satellite a, which is ascribed to the $4f$ state of trivalent Ce ion as described later. Hence, we attribute the main enhancement of the feature b to the Ce $4f$ state of CeO_2. The CIS spectrum of the feature c shows a shoulder at 128 eV as well as small enhancement at 124 eV. This suggests that the feature c includes other components than the $4f$ state. In other words, the CIS spectrum of the feature c may show the enhancement due to the Ce $5d$ component in the valence band. If this is the case, judging from the profiles of the CIS spectrum of the feature b and the off-resonance EDC, the Ce $5d$ component might contribute to the enhancement of the feature b by at most 30% of the total enhancement at the 124-eV photoexcitation. However, we again emphasize that the asymmetric profile of the CIS spectrum of the feature b reveals the resonant enhancement due to the $4f$ electron.

The CIS spectrum for the weak satellite a on the low binding-energy side of the main feature b is quite similar to that for the Ce $4f$ state in Ce trihalides.[26] The maximum of this CIS spectrum is located at 121 eV and the same multiplet structures as those in Ce trihalides are observed in the prethreshold region. Thus, we ascribe the satellite a to the $4f$ state of a trivalent Ce ion, which might exist on a sample surface or near an oxygen-defect site. The satellite d shows weak enhancement. However, the enhancement at 124 eV appears to be caused by the secondary electrons of the main band b, as described later. The feature d might be ascribed to the oxygen defect in CeO_2. At present, its origin is not clarified yet.

The asymmetric enhancement in the $4d \rightarrow 4f$ giant-absorption region gives an evidence that the $4f^1\underline{L}$ configuration exists in the ground state and that CeO_2 is certainly mixed valent between the $4f^0$ and $4f^1\underline{L}$ configurations. Corresponding to the mixed valence in the ground state, the $4f^0\underline{L}$ and $4f^1\underline{L}^2$ final configurations will exist in the valence-band photoemission of CeO_2. For the $4f^0\underline{L}$ final configuration, the indirect process through the super Coster-Kronig decay of the $4d^94f^2\underline{L}$

intermediate state reached by the $4d \rightarrow 4f$ transition causes strong resonant enhancement of the $4f$ photoemission. On the other hand, the $4f^1\underline{L}^2$ final configuration would show resonant enhancement through the super Coster-Kronig transition from the $4d^9 4f^3\underline{L}^2$ intermediate state, if the $4d^9 4f^3\underline{L}^2$ intermediate state could be reached directly from the $4f^2\underline{L}^2$ configuration in the ground state or through the hybridization between the $4d^9 4f^2\underline{L}$ and $4d^9 4f^3\underline{L}^2$ configurations. Actually, the $4f^2\underline{L}^2$ configuration is hardly considered to exist in the ground state because of the large Coulomb interaction between the $4f$ electrons, and the hybridization effects in the intermediate state may be very small because of a large energy difference between the $4d^9 4f^2\underline{L}$ and $4d^9 4f^3\underline{L}^2$ configurations. It is also expected that the super Coster-Kronig process predominates over the other Auger decay processes. Thus, we consider that the feature *b* is mainly composed of the $4f^0\underline{L}$ final configuration, while the feature *c* has a component of the $4f^1\underline{L}^2$ final configuration.

The Ce $4f$ photoemission may be enhanced at the photoexcitation to the $4d^9 4f^2\underline{L}$ excited state. In fact, we notice that the CIS spectrum of the feature *b* in the prethreshold region shows weak humps at 108 and 115 eV, though the enhancement at 108 eV is not so strong compared with the TY spectrum. This can be explained by the fact that the absorption band at 115 eV corresponds to the transition to the $4d^9 4f^2\underline{L}$ states, while the peak at 108 eV corresponds to the transition to the $4d^9 4f^1$ excited state hybridized with the $4d^9 4f^2\underline{L}$ state.

In order to clarify the spectral distribution of the $4f$ state in CeO_2, we compare the valence-band EDC on resonance (124.5 eV) with that off resonance (117.0 eV) in Fig. 6. Here, we subtracted the background due to secondary electrons from the measured EDC's by a method in Ref. 21. For comparison between the on- and off-resonance EDC's, we should take account of the dependence of the ionization cross sections of the nonresonant components on the photon energy and that of the transmittance of the DCMA on the kinetic energy of incident photoelectrons, i.e., on the photon energy. We assumed that these dependences are represented by a smooth broken line as shown in Fig. 4. The off-resonance EDC is corrected by multiplying the ratio of the intensity assumed by the broken line at 124.5 eV to that at 117 eV. Then we obtain a difference spectrum by subtracting the corrected off-resonance EDC from the on-resonance EDC. In this difference spectrum, the contribution of the Ce $5d$ electrons may still remain. However, as already mentioned, the Ce $5d$ component, if any, is smaller than 30% of the peak intensity of the difference spectrum. Thus, the main part of the difference spectrum represents the $4f$ partial density of states in CeO_2, while the corrected off-resonance EDC mainly gives distribution of the nonresonant component.

It is remarkable that the difference spectrum exhibits a single peak rather than a double-peak structure such as reported in Ce trihalides[30,34] and many Ce compounds.[17] With a simple consideration, the energy separation and the hybridization between the $4f^0\underline{L}$ and $4f^1\underline{L}^2$ final configurations are expected to nearly equal those between

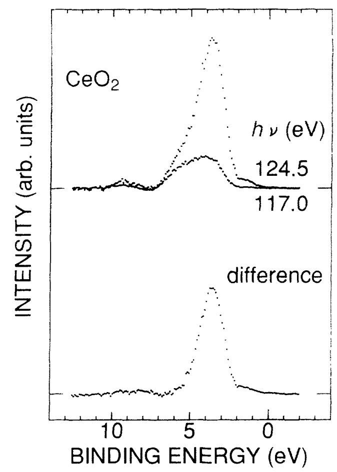

FIG. 6. Energy distribution curves in the valence-band region for a CeO_2 film measured at photon energies on- (124.5 eV) and off- (117.0 eV) resonances, and a difference spectrum between these curves.

the $4f^0$ and $4f^1\underline{L}$ configurations in the ground state with the average $4f$ electron number of 0.5. Consequently, both the bonding and antibonding states of these final configurations will have almost the same $4f^0\underline{L}$ component. The $4f$ photoemission in CeO_2 is also expected to show two peaks of almost the same intensity corresponding to the bonding and antibonding states of the final configurations. The discrepancy between the observation and the above simple expectation may be explained by taking account of the width of the O $2p$ valence band. Or it might be explained by the inclusion of the $4f^9 4f^3\underline{L}^2$ intermediate states. On the other hand, the energy-band calculation[9] shows that the bottom and upper parts of the O $2p$ band contain the Ce $5d$ and Ce $4f$ characters, respectively. The peak of the difference spectrum is located on the low binding-energy side of the valence band as seen in Fig. 6. This seems to correspond to the result of the energy-band calculation.

C. 5*p* emission

Figure 7 shows a series of detailed EDC's in the Ce $5p$ region measured at various photon energies for the CeO_2 evaporated film in comparison with results of LaF_3 and CeF_3. The Ce $5p$ band in CeF_3 is broader than the La $5p$ band in LaF_3, which suggests the interaction between the $5p$ hole and $4f$ electron. The Ce $5p$ band in CeO_2 is much broader and shows more features, at least three as labeled by $e-g$, than those in LaF_3 and CeF_3. One of possible origins is that the O $2s$ band overlaps with the Ce $5p$ band. On the assumption that the energy separation between the O $2p$ and O $2s$ levels in CeO_2 is the same as those in the other rare-earth oxides, 16.7 eV[1], the O $2s$ level is considered to be located between the features *f* and *g*. However, as seen in Fig. 5, all the CIS spectra obtained at binding energies of the features $e-g$ show reso-

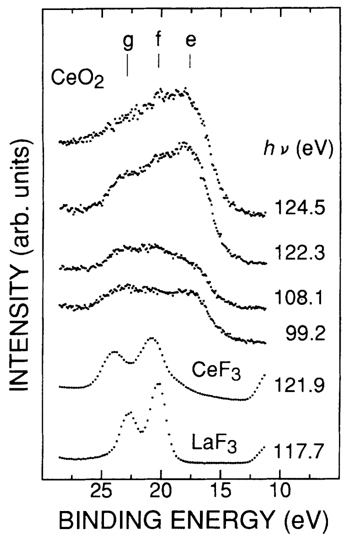

FIG. 7. Energy distribution curves in the Ce 5*p* band region for a CeO_2 film measured at various photon energies in comparison with the lanthanide 5*p* photoemission spectra of LaF_3 and CeF_3.

nant enhancement in the giant-absorption region and they are very similar to each other. Thus, we consider that the contribution of the O 2*s* level is not so large for the features *e*–*g* and ascribe all of the features to the Ce 5*p* bands.

We find that the features *g* and *f* are pronounced in the EDC measured at the 108.1-eV photoexcitation compared with the feature *e*. This aspect is also seen in the CIS spectra in Fig. 5 as the enhancement at 108 eV. On the other hand, the feature *e* shows weak enhancement around 115 eV, while the feature *g* does not. These results can be explained by the mixed-valent nature of CeO_2. The $5p^54f^0$ and $5p^54f^1\underline{L}$ configurations in the final state will appear corresponding to the $4f^0$ and $4f^1\underline{L}$ configurations in the ground state. Since it is considered that the $5p^54f^0$ and $5p^54f^1\underline{L}$ final configurations are enhanced at the photoexcitation to the $4d^94f^1$ and $4d^94f^2\underline{L}$ excited states, respectively, the feature *e* is ascribed to the $5p^54f^1\underline{L}$ final configuration and the features *f* and *g* to the $5p^54f^0$ one. Furthermore, the fact that the features *f* and *g* are enhanced at the 108-eV photoexcitation suggests that these features include the $5p_{1/2}$ component, since the La $5p_{1/2}$ photoemission in La trihalides shows selective resonant enhancement at the $^3D_1$ photoexcitation.[24,25] According to recent theoretical studies,[10–15,35] the energy separation between the $4f^0$ and $4f^1\underline{L}$ configurations is 1.5 eV and the Ce 5*p* core-hole potential, which acts on the 4*f* electron, is 3.75 eV in CeO_2. If the interaction in the final state is neglected, it is estimated that the $5p^54f^1\underline{L}$ state lies about 2.25 eV below the $5p^54f^0$ state. In addition, the spin-orbit splitting of the Ce 5*p* levels in Ce trihalides is 2.9 eV. These energy separations show reasonable agreement with those among the features *e*–*g*. Thus, the feature *f* is composed of two configurations $\underline{5p}_{1/2}4f^1\underline{L}$ and $\underline{5p}_{3/2}4f^0$. Here, $\underline{5p}_j$ indicates a hole in the $5p_j$ sublevel. Consequently, we assign features *e*, *f*, and *g* to the $\underline{5p}_{3/2}4f^1\underline{L}$, $\underline{5p}_{1/2}4f^1\underline{L}+\underline{5p}_{3/2}4f^0$, and $\underline{5p}_{1/2}4f^0$ final configurations, respectively.

The $N_{4,5}O_{2,3}V$ Auger peak may cross Ce 5*p* bands near 108 eV as indicated by the arrow *B* in Fig. 3. However, it is considered that the 4*d* hole decays dominantly through the direct recombination in the prethreshold region.[24] The intraatomic decay processes in the direct recombination, i.e., $4d^94f^1 \rightarrow 5p^54f^0+\epsilon l$ and $4d^94f^2\underline{L} \rightarrow 5p^54f^1\underline{L}+\epsilon l$ are expected to predominate over the interatomic processes. Thus, it is reasonable to ignore the interatomic processes in the above discussion.

IV. CONCLUSION

The 4*f* electron state and the decay process of the $4d^94f^{n+1}$ excited states in CeO_2 are investigated with the use of a resonant photoemission technique in the Ce $4d \rightarrow 4f$ photoabsorption region. Although the valence-band photoemission spectra measured at the off-resonance photon energies exhibit a single emission band as observed in XPS studies, the 4*f* emission is derived by the resonant photoemission. This fact gives an evidence that CeO_2 is certainly mixed valent between the $4f^0$ and $4f^1\underline{L}$ configurations in the ground state. The extracted 4*f* spectrum shows a single-peak distribution rather than such a double-peak structure as observed in Ce trihalides, which is in contrast to the simple speculation along the cluster model. Further theoretical investigation will be necessary to explain the present observation.

The Ce 5*p* photoemission band in CeO_2 spreads over 10 eV and has at least three or more features, which are ascribed to the mixed-valent nature of CeO_2. These features show photon-energy dependences different from each other in the prethreshold region and are ascribed to the $\underline{5p}_{3/2}4f^1\underline{L}$, $\underline{5p}_{1/2}4f^1\underline{L}+\underline{5p}_{3/2}4f^0$, and $\underline{5p}_{1/2}4f^0$ configurations. We also find that the $4d^94f^{n+1}$ excited state in CeO_2 tends to decay selectively to the $\underline{5p}_{1/2}$ final state at photoexcitation including the $^3D_1$ of the $4d^94f^1$ state as observed in La trihalides. We confirm that the absorption lines in the prethreshold region of CeO_2 are explained by the theoretical expectation by Kotani *et al.*[15] Especially, we clearly observe the absorption feature due to the transition to the $4d^94f^2\underline{L}$ excited state, which was ambiguous in the previous measurements.

ACKNOWLEDGEMENTS

The authors would like to appreciate the staff members of Synchrotron Radiation Laboratory, the Institute for Solid State Physics, the University of Tokyo, for their support during the course of this experiment. They also would like to thank Professor A. Kotani and Dr. H. Ogaswara for valuable discussions.

[1]A. F. Orchard and G. Thornton, J. Electron. Spectrosc. Relat. Phenom. **10**, 1 (1977).
[2]M. V. Ryzhkov, V. A. Gubanov, Yu. A. Teterin, and A. S. Baev, Z. Phys. B. **59**, 1 (1985).
[3]J. W. Allen, J. Magn. Magn. Mater. **47-48**, 168 (1985).
[4]E. Wuilloud, B. Delley, W.-D. Schneider, and Y. Baer, Phys. Rev. Lett. **53**, 202 (1984).
[5]R. Haensel, P. Rabe, and B. Sonntag, Solid State Commun. **8**, 1845 (1970).
[6]T. M. Zimkina and I. I. Lyakhaovskaya, Fiz. Tverd. Tela (Leningrad) **18**, 1143 (1976) [Sov. Phys. Solid State **18**, 655 (1976)].
[7]T. Hanyuu, H. Ishii, M. Yanagihara, T. Kamada, T. Miyahara, H. Kato, K. Naito, S. Suzuki, and T. Ishii, Solid State Commun. **56**, 381 (1985).
[8]T. Miyahara, A. Fujimori, T. Koide, S. Sato, S. Shin, M. Ishigame, Y. Ōnuki, and T. Komatsubara, J. Phys. Soc. Jpn. **56**, 3689 (1987).
[9]D. D. Koelling, A. M. Boring, and J. H. Wood, Solid State Commun. **47**, 227 (1983).
[10]A. Kotani, H. Mizuta, T. Jo, and J. C. Parlebas, Solid State Commun. **53**, 805 (1985).
[11]A. Kotani, T. Jo, and J. C. Parlebas, Adv. Phys. **37**, 37 (1988).
[12]A. Fujimori, Phys. Rev. B **28**, 2281 (1983).
[13]T. Nakano, A. Kotani, and J. C. Parlebas, J. Phys. Soc. Jpn. **56**, 2201 (1987).
[14]T. Jo and A. Kotani, Phys. Rev. B **38**, 830 (1988).
[15]A. Kotani, H. Ogasawara, K. Okada, B. T. Thole, and G. A. Sawatzky, Phys. Rev. B **40**, 65 (1989).
[16]M. Taniguchi, A. Fujimori, and S. Suga, Solid State Commun. **70**, 191 (1989).
[17]J. W. Allen, S.-J. Oh, O. Gunnarsson, K. Schönhammer, M. B. Maple, M. S. Torikachvili, and I. Lindau, Adv. Phys. **35**, 275 (1986).
[18]K. Soda, T. Mori, M. Taniguchi, S. Asaoka, K. Naito, Y. Ōnuki, T. Komatsubara, T. Miyahara, S. Sato, and T. Ishii, J. Phys. Soc. Jpn. **55**, 1709 (1986).
[19]T. Ishii, K. Soda, K. Naito, T. Miyahara, H. Kato, T. Mori, M. Taniguchi, A. Kakizaki, Y. Ōnuki, and T. Komatsubara, Phys. Scr. **35**, 603 (1987).
[20]A. Kakizaki, T. Kinoshita, T. Kashiwakura, T. Okane, S. Suzuki, S. Sato, Y. Isikawa, K. Soda, T. Mori, and T. Ishii, in *Physical Properties of Actinide and Rare Earth Compounds, JJAP Series 8,* edited by T. Kasuya, T. Ishii, T. Komatsubara, O. Sakai, N. Mōri, and T. Saso (Publication Office, Jpn. J. Appl. Phys., Tokyo, 1993), p. 85.
[21]K. Soda, T. Mori, Y. Ōnuki, T. Komatsubara, S. Suga, A. Kakizaki, and T. Ishii, J. Phys. Soc. Jpn. **60**, 3059 (1991).
[22]S. Suzuki, S. Sato, T. Ejima, K. Murata, Y. Kudo, T. Takahashi, T. Komatsubara, N. Sato, M. Kasaya, T. Suzuki, T. Kasuya, S. Suga, H. Matsubara, Y. Saito, A. Kimura, K. Soda, Y. Ōnuki, T. Mori, A. Kakizaki, and T. Ishii, in *Physical Properties of Actinide and Rare Earth Compounds, JJAP Series 8,* edited by T. Kasuya, T. Ishii, T. Komatsubara, O. Sakai, N. Mori, and T. Saso (Publication Office, Jpn. J. Appl. Phys., Tokyo, 1993), p. 59.
[23]R. D. Cowan, *The Theory of Atomic Structure and Spectra* (University of California Press, Berkeley, 1981), p. 526.
[24]K. Ichikawa, O. Aita, K. Aoki, M. Kamada, and K. Tsutsumi, Phys. Rev. B **45**, 3221 (1992).
[25]H. Ogasawara, A. Kotani, B. T. Thole, K. Ichikawa, O. Aita, and M. Kamada, Solid State Commun. **81**, 645 (1992).
[26]K. Soda, Y. Taguchi, M. Matsumoto, A. Tabata, K. Hatauchi, T. Umehara, S. Tanaka, K. Ichikawa, and O. Aita, Phys. Rev. B (to be published).
[27]S. Suzuki, T. Ishii, and T. Sagawa, J. Phys. Soc. Jpn. **37**, 1334 (1974).
[28]E. Paparazzo, Surf. Sci. Lett. **234**, 253 (1990).
[29]W. Gudat and C. Kunz, Phys. Rev. Lett. **29**, 169 (1972).
[30]A. Fujimori, T. Miyahara, T. Koide, T. Shidara, H. Kato, H. Fukutani, and S. Sato, Phys. Rev. B **38**, 7789 (1988).
[31]J. M. Lawrence, A. J. Arko, J. J. Joyce, R. I. R. Blyth, R. J. Bartlett, P. C. Canfield, Z. Fisk, and P. S. Riseborough, Phys. Rev. B **47**, 15 460 (1993).
[32]A. Zangwill and P. Soven, Phys. Rev. Lett. **45**, 204 (1980).
[33]M. Richter, M. Meyer, M. Pahler, T. Prescher, E. v. Raven, B. Sonntag, and H.-E. Wetzel, Phys. Rev. A **39**, 5666 (1989).
[34]K. Okada and A. Kotani, in *Core-Level Spectroscopy in Condensed Systems,* edited by J. Kanamori and A. Kotani (Springer-Verlag, Berlin, 1987), p. 64.
[35]S. Tanaka and A. Kotani, J. Phys. Soc. Jpn. **61**, 4212 (1992).